ELSEVIER
CrossMark
Available online at www.sciencedirect.com
ScienceDirect
Procedia Engineering 147 (2016) 104 – 109
Procedia Engineering
www.elsevier.com/locate/procedia

11th conference of the International Sports Engineering Association, ISEA 2016

PIV Measurement of a Flying Table Tennis Ball

Yasufumi KONISHI*, Hiroyuki OKUIZUMI, Tomoyuki OHNO

Institute of Fluid Science, Tohoku Univarsity, Aobaku, Katahira 2-1-1, Sendai, Miyagi 980-8577, Japan

Abstract

There are some reports that the Magnus force becomes negative at some situation in wind tunnel test. If so, there is possibility of a variety of curves using change of the direction of the Magnus force. PIV measurements of a flying table tennis ball were conducted to confirm whether a similar phenomenon was observed in real flight. A high-speed camera with a frame rate of 10k fps was used to capture the instantaneous flow field of the flying ball. The imaging region was 210 mm × 210 mm. The Reynolds number was approximately 6.5×10^4, which corresponds to a smash in table tennis. A coordinate transformation of the ball's fixed coordinate system captured the wake motion of non-rotating and rotating balls. In the non-rotating condition, the averaged velocity field of the ball was observed to be symmetric, whereas, in the rotating condition, it was asymmetric, which shows the Magnus effect. At spin parameter is 0.65, the Magnus force becomes zero to indicate the appearance of the negative Magnus force. These observations quantitatively agree with the wind tunnel test.

Peer-review under responsibility of the organizing committee of ISEA 2016
Keywords: Magnus force; PIV; table tennis; sphere

1. Introduction

In a ball game, the Magnus force is commonly used to change the traveling direction by adding spin to the ball. Because of the low density and mass of a table tennis ball, a variety of spins are possible and the direction change is large. Therefore, the Magnus force plays an important role in table tennis. The Magnus force is a result of pressure differences at the both sides of the ball. In some situations, the ball's direction change is opposite. This is called the negative Magnus force and was first reported by Maccoll [1]. Multiple studies have been conducted to identify the domain where the negative Magnus force occurs and to reveal its associated phenomena [2-5]. Figure 1 shows such a domain in the plane of the Reynolds number, Re, and the Spin parameter, SP, which is defined as the ratio of the peripheral velocity and the freestream velocity. The Reynolds number is defined by the diameter of the sphere and the freestream velocity. Our previous study [2] and a prediction by Kim et al. [3] nearly coincided with Taneda's result [4] at a critical Reynolds number of approximately 5.5×10^4. This domain contains the conditions of a smash, which Reynolds number is around 5.8×10^4 to 7.3×10^4 and spin parameter is around 0.22 to 0.49, in a table tennis game [6]. Muto et al. [4] conducted large eddy simulations at high Reynolds number 2.0×10^5 and showed that the negative Magnus force was related to the boundary layer transition on both sides of the rotating sphere. This was also suggested by Kim et al. [3] from PIV measurements. However, force estimations from the trajectory of the ball indicated that the negative Magnus force domain shifts toward higher Reynolds numbers of approximately 8.0×10^4 or more [7, 8]. This difference is so large that it cannot be explained by the accuracy of the flight tests alone. No study has ever attempted to determine the origin of these differences. As a first step, we conducted a time-resolved PIV measurement of a flying table tennis ball to compare the flow field between the wind tunnel and flight tests.

* Corresponding author. Tel.: +81-22-217-5898; fax: +81-22-217-5280.
E-mail address: konishi@edge.ifs.tohoku.ac.jp

Peer-review under responsibility of the organizing committee of ISEA 2016
doi:10.1016/j.proeng.2016.06.197

Nomenclature

Re	Reynolds number
SP	spin parameter
U	velocity of the ball
u	velocity component of traveling direction
d	diameter of the ball
V	peripheral velocity
r	radius of the ball
ν	viscosity of the air
ω	angular velocity

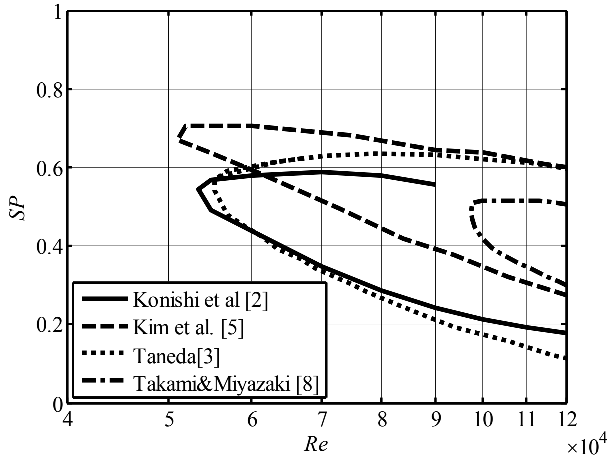

Fig. 1. Region of the negative Magnus force in the *Re*–*SP* plane.

2. Experimental Setup and Procedure

Figure 2 illustrates the setup of the PIV measurements. In the flight test, the surrounding atmosphere should be calm. Because

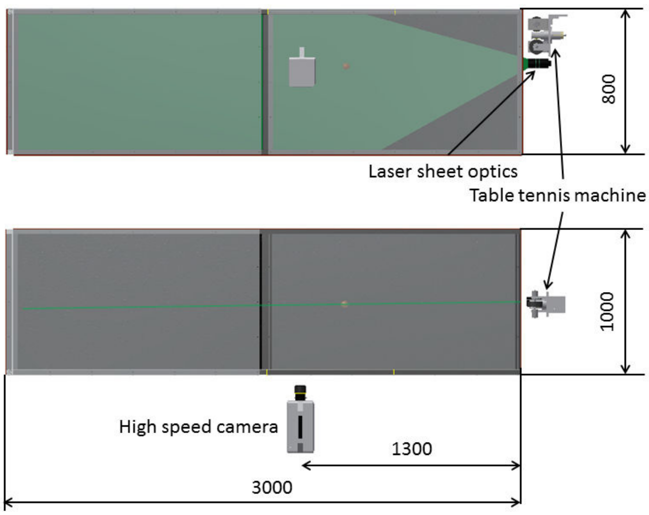

Fig. 2. Sketch of the experimental setup (dimensions in mm).

the weight of the experimental table tennis ball is only 2.4 g, the air flow in the surrounding atmosphere have a large effect on the measurements. The flight path was within a large closed cargo made of an acrylic plate and a hard board with a length of 3.0 m, height of 1.0 m, and width of 0.8 m. This setup helped us maintain the surrounding atmosphere to be calm and a constant density of particles for the PIV measurement.

The ball that we used is called a "large ball" and has a diameter of 44 mm, which is somewhat larger than the national official standard of 40 mm; the ball's mass was 2.4 g, which is somewhat lighter than the national official standard of 2.7 g. This type of ball is typically used by beginners or seniors for recreational use and has become common in Japan and Asia-Pacific. Except for its size and mass, it is made using the same processes and precision as an official ball. To avoid halation of the ball, the ball was splayed with a red fluorescent paint, and the letter "A" was painted on the ball as a marker to detect the rotation.

The ball was shot from a custom-made two-rotor-type table tennis machine. The diameter of each rotor was 90 mm. The initial speed and spin rate of the ball were controlled by changing the rotation speed of each rotor separately. PWM signals for changing the rotation speed of the rotors were generated and controlled using NI LabVIEW 2010.

Two-dimensional time-resolved PIV measurements were conducted in the central plane of the ball in the flying path, as shown in Fig. 2. A high-speed camera (Fastcam SA-X2, Photron) and a high repetition-rate pulsed YLF laser (DM30-527DH, Photonics Industries) were synchronized via a synchronizer (BNC-575, BNC). The laser sheet was introduced from just under the table tennis machine. Therefore, we could not observe the front of the flying ball. The particles, with a mean diameter of approximately 1 μm, were generated using a Laskin-nozzle-type seed generator (PivPart45, PivTec). The imaging region was 210 mm × 210 mm with a 1024 × 1024 px and 12-bit resolution. The repetition rate of the camera and laser was 10 kHz. Therefore, the PIV data were obtained at 10 kHz, and the time between the pulses was 100 μs. The start time of the measurements was acquired from a simple trigger module comprising a photodiode sensor and an infrared laser. The vector calculation was performed using commercial software (Dynamic studio 2015, Dantec Dynamics).

The Reynolds number, *Re*, and spin parameter, *SP*, are defined in Eqs. 1 and 2.

$$Re = \frac{Ud}{\nu} \tag{1}$$

$$SP = \frac{V}{U} = \frac{r\varpi}{U} \tag{2}$$

The flying speed, U, and the diameter of the ball, d , were chosen as the characteristic velocity and length, respectively. The flying speed, U, is the initial velocity in the imaging region. The angular velocity, ω, was manually identified from the change in the angle between the captured images.

3. Experimental result

Figures 3(a) and (b) show the particle image and the calculated instantaneous vector map at the launch condition for (*Re*, *SP*) = (7.6 × 10^4, 0.75). In this figure, the ball rotates counterclockwise. As seen in Fig. 3(a), almost the entire region around the ball except the front of the ball was visualized because the laser sheet was introduced from behind the ball. The letter "A" can be seen, which is a marker to measure the rotation speed. The vector map shows a zigzag formation of the flow behind the ball. This indicates that the pressure behind the ball was low and that the low-pressure region was swinging.

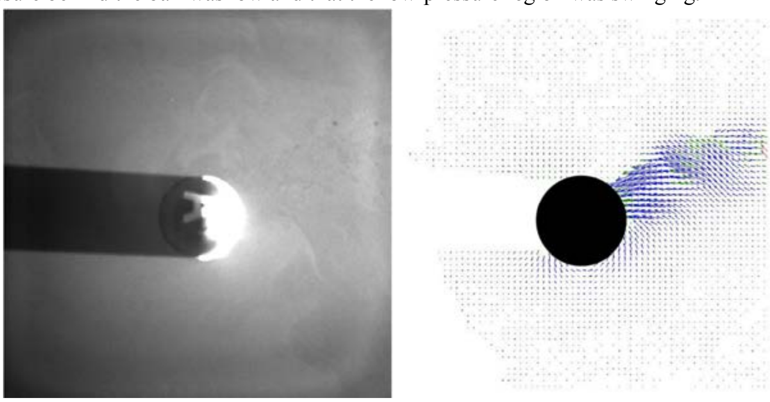

Fig. 3. (a) Captured image; and (b) instantaneous vector field at the initial conditions of (Re, SP) = (7.6 × 10^4, 0.75). The colors of the vectors, blue, green, or red, show the correct, substituted, or rejected vectors, respectively.

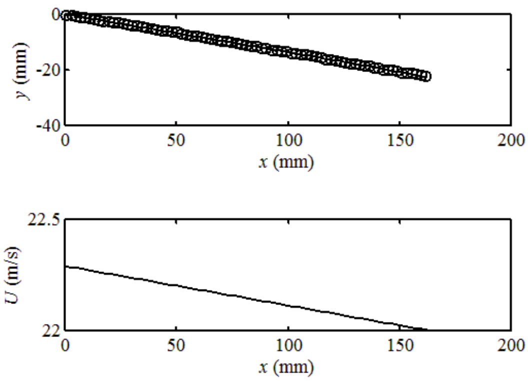

Fig. 4. (a) Trajectory of the table tennis ball with an initial condition of (*Re*, *SP*) = (7.6 × 104, 0.75). The circles show the extracted position, and line shows the fitting curve. (b) The velocity of the ball at each location.

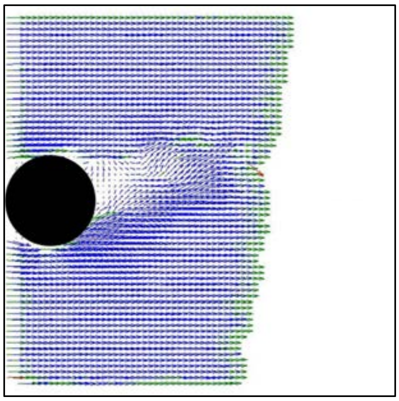

Fig. 5. Coordinate transformed instantaneous vector filed with the initial condition of (*Re*, *SP*) = (7.6 × 104, 0.75). The color of the vectors is the same as Fig. 3 (b).

To reveal these flow motions more clearly, the coordinates were converted into a moving coordinate system. The position of the ball in the frame was identified using the Hough transformation [9]. The result is presented in Fig. 4. In Fig. 4(a), the origin of the coordinate system was chosen as the center of the ball, where the entire sphere entered into the imaging region. The line was obtained by least squares fitting. The direction and movement of the ball was calculated and translated from this flight path.

Figure 4(b) represents the change of the flying speed of the ball. It is important to note that the flying speed of the table tennis ball decreased gradually; however, the rotational speed did not change. At this launch condition, (*Re*, *SP*) = (7.6 × 10^4, 0.75), the flying speed was decreased from 22.3 m/s to 22.0m/s while angular velocity remain constant 900 rad/s, which corresponds to *Re* = 6.3 × 10^4 and *SP* = 0.89. The increase in SP was because of the deceleration of the flight velocity, which, in turn, was because of the light weight of the table tennis ball.

Figure 5 shows the velocity vector map in the moving coordinate system. Because of the changing the position of the ball, the area to the right of the figure has no vectors. The wake of the ball meanders and the direction of the wake moves upward in the downstream direction, which indicates that the lift force is downward. This is the well-known Magnus force.

The experiment was conducted 10–11 times for each initial condition in order to obtain the averaged ensemble flow field. Table 1 lists the results of *Re* and *SP* for each trial of the initial conditions. As previously mentioned, the speed of the ball decreases rapidly while the rotational speed is maintained. The averaged ensemble flow field was obtained for each initial condition. The grayed out cells indicate that the value exceeded the average value by more than 5%; trials with such values were excluded from calculations of the averaged ensemble data.

Table 1. Reynolds number and Spin parameter of each trial. The average data was obtained excluding the grayed out values.

(*Re*, *SP*)	(7.8 × 10^4, 0.0)	(7.8 × 10^4, 0.25)		(7.8 × 10^4, 0.4)		(7.6 × 10^4, 0.6)		(7.6 × 10^4, 0.75)	
No	*Re*	*Re*	*SP*	*Re*	*SP*	*Re*	*SP*	*Re*	*SP*
No1	62943	62961	0.26	60739	0.46	63770	0.71	66923	0.82
No2	66518	63775	0.25	60300	0.46	63877	0.71	63421	0.89
No3	64602	67048	0.27	62376	0.48	63567	0.61	69068	0.83
No4	63955	65528	0.27	70032	0.43	58298	0.67	61293	0.92
No5	63058	63268	0.25	63085	0.48	63680	0.67	68408	0.81
No6	65080	64627	0.29	64264	0.49	66794	0.59	67934	0.85
No7	64371	63386	0.28	63442	0.5	61675	0.66	62166	0.9
No8	58512	68633	0.22	68043	0.48	67720	0.62	68131	0.85
No9	62742	63772	0.3	70351	0.43	65864	0.56	63530	0.88
No10	64855	63735	0.28	69188	0.44	64446	0.64	73845	0.75
No11		65386	0.25			64484	0.65		
average	6.4 × 10^4	6.4 × 10^4	0.27	6.5 × 10^4	0.47	6.4 × 10^4	0.65	6.6 × 10^4	0.86

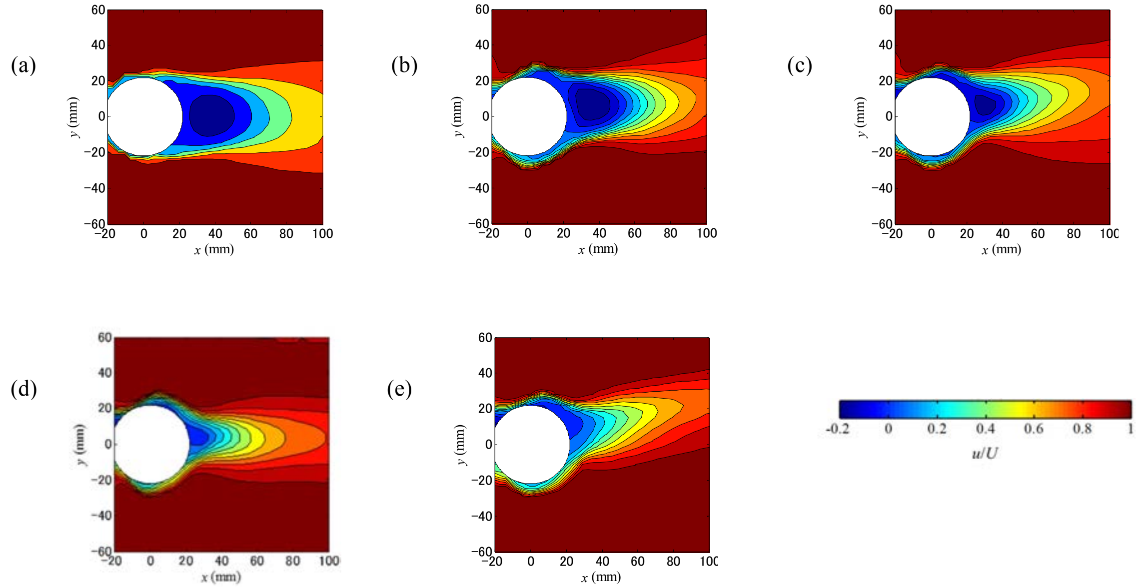

Fig. 6. Averaged velocity contour map of the traveling direction: (a) (Re, SP) = (6.4 × 10^4, 0.0); (b) (Re, SP) = (6.4 × 10^4, 0.27); (c) (Re, SP) = (6.5 × 10^4, 0.47); (d) (Re, SP) = (6.4 × 10^4, 0.65); and (e) (Re, SP) = (6.6 × 10^4, 0.86).

Figure 6 illustrates the contour of the averaged velocity component of the traveling direction. The wake of the ball is symmetric for the non-rotating condition, SP = 0.0. As the rotational speed increases, the upward-inclined wake suggests that the Magnus force becomes large, except at SP = 0.65. At the condition of SP = 0.65, the wake appears nearly symmetric. This indicates that the Magnus force decreases at this point to nearly zero. This phenomenon was observed in force measurement tests in a wind tunnel [2,5]. However, there was a slight difference between the flight and wind tunnel tests in that the Magnus force became negative in the wind tunnel tests. For this phenomenon, the laminar-turbulent transition at the boundary layer and the separation play important roles. The boundary layer of the both side is considered to be laminar at this low Reynolds number. At low SP , SP = 0.27 in this experiments, the separation point of the lower side boundary layer goes downstream and the separation point of the upper side goes upstream compared with the no-rotation condition, SP = 0.0, due to increase of peripheral velocity. As the result, the wake becomes upward-inclined and it suggests that the Magnus force is positive. The upward inclined angle increases with increase of the spin parameter as can be seen in the case of SP = 0.47. As increase the SP more, the separated flows of upper side becomes turbulence and reattach to the surface of the ball causes the relation between separation points of the upper side boundary layer and lower side boundary layer change to inverse. Thus the Magnus force becomes negative. It was observed at SP = 0.65 in this experiment as already mentioned before. For more increased SP, SP = 0.86 in this experiment, the boundary layer transition of lower side boundary layer occurs. For more increased SP, SP = 0.86 in this experiment, the boundary layer transition of lower side boundary layer occurs. Then the relation between these separation points becomes usual pattern again. The results indicate that the critical Reynolds number and spin parameter of the negative Magnus force in this flight experiments are around 6.4×10^4 and 0.65 respectively. These values are slightly higher than the critical value obtained from the our previous wind tunnel test [2] but closer than the critical value obtained from the trajectory of the ball in flight tests [7, 8]. The lift and drag coefficient from the trajectory of the ball in flight tests are estimated with an assumption that these values are remain constant in whole region of the trajectory. And the Reynolds number is defined by the launch condition. It seems that these assumptions make large difference between wind tunnel and flight tests.

4. Conclusions

There are differences in the aerodynamic forces between wind tunnel tests and actual flying balls with rotation. To elucidate the reasons for these differences, we conducted a time-resolved PIV on a flying table tennis ball.

Owing to the increased sensitivity of the high-speed camera, the time-resolved PIV measurements could be performed at a resolution of 1024 × 1024 px with 10 kfps. The averaged velocity field reveals that the wake behind the ball with no rotation, SP = 0.0, is symmetric in the observed plane.

These phenomena qualitatively agree with the results from the wind tunnel tests. The critical Reynolds number and spin parameter obtained from this flight test are $Re = 6.4 \times 10^4$ and SP = 0.65 respectively.

Acknowledgements

This work was partially supported by the Japan Society for the Promotion of Science (JSPS), a Grant-in-Aid for Young Scientists (B), No. 25870065.

References

[1] Maccoll, J. H., "Aerodynamics of a spinning sphere," J. Roy. Aero. Soc., 32, 1928, 777-798.
[2] Konishi, Y., Itami, T. Okuizumi H., Ohno, T., Obayashi, S., Region of the Negative Magnus Force on Rotating Sphere, ICFD9, 2012, USB.
[3] Kim J., Choi H., Park H., Yoo J. Y., Inverse Magnus effect on a rotating sphere: when and why, F. Fluid Mech. 752, R2, 2014, doi:10.1017.
[4] Taneda S., Negative Magnus effect, Reports of Research Institute for Applied Mechanics, Vol. 5 No. 20 (1957), pp. 123-128.
[5] Muto M., Tsubokura M., and Oshima N., Negative Magnus lift on a rotating sphere at around the critical Reynolds number, Physics of Fluids, Vol. 24, No. 1 (2012), 014102.
[6] Wei X., The C., Qin Z., Speed and spin of 40 mm table tennis ball and the effects on elite players, 20th Int. Symp. Biomecanics in Sports, 2002, 623-626.
[7] Konishi Y., Okuizumi H., Ohno H., A comparison of the aerodynamic force of table tennis ball between wind tunnel experiment and a lfght experiment., SHD2014, 2014, USB. (in Japanese)
[8] Takami K., Miyazaki T., Himeno R., Negative Magnus Force Exerted on a Back-spinning Spherical Body ～Measurement by Flight Experiments～, Nagare, 28, 2009, 347-356. (in Japanese)
[9] Yuen, H.K., Princen, J., Illingworth, J. and Kittler, J., Comparative study of Hough transform methods for circle finding, Image and Vision Computing. Vol. 8, No. 1, 1990, 71-77.